

A Novel Method for Numerical Analysis of 3D Nonlinear Thermo-Mechanical Bending of Annular and Circular Plates with Asymmetric Boundary Conditions Using SAPM

A.R. Golkarian¹, M. Jabbarzadeh^{2,*}, Sh. Dastjerdi³

¹Department of Mechanical Engineering, Science & Research Branch, Islamic Azad University, Tehran, Iran

²Department of Mechanical Engineering, Mashhad Branch, Islamic Azad University, Mashhad, Iran

³Department of Mechanical Engineering, Shahrood Branch, Islamic Azad University, Shahrood, Iran

Received 30 March 2019; accepted 26 May 2019

ABSTRACT

This study is the first report of numerical solution of nonlinear bending analysis for annular and circular plates based on 3D elasticity theory with asymmetric boundary conditions using semi-analytical polynomial method (SAPM). Orthotropic annular and circular plates are subjected to transverse loading and 3D bending analysis in the presence of symmetric and asymmetric boundary conditions is studied. For asymmetry cases, the plate boundaries are divided to two or three parts and various boundary conditions such as clamped, simply supported and free edges are defined for each part. The asymmetry in one and two directions is studied. The influence of elastic foundations, mechanical and thermo-mechanical loadings are examined. Regarding this fact that no study has been done in the case of asymmetric boundary conditions, the obtained results are compared with FEM results by ABAQUS. The results show good agreement with the literatures and FEM results, which it shows that the presented method can use to analyze the 3D bending of plates under asymmetric conditions. In addition, it is observed that 3D elasticity estimates some higher deflections than other theories. However, the obtained results by 3D elasticity theory and those obtained by FEM analysis in the case of asymmetric conditions are so close.

© 2019 IAU, Arak Branch. All rights reserved.

Keywords: 3D elasticity, SAPM, Annular plates, Nonlinear bending, Asymmetry.

1 INTRODUCTION

DURING last decades, different studies are devoted to analyze the bending behavior of plates with different shape, mechanical behavior, boundary conditions and type of loading based on different plate theories. Different classical plate theories are proposed to use in this way. The basic difference between these theories is the way of displacement field definition or may be better to say, their employed assumptions. The simplest and oldest

*Corresponding author. Tel.: +98 513 6625046; Fax: +98 513 6625046.
E-mail address: jabbarzadeh@mshdiau.ac.ir (M. Jabbarzadeh).

theory is the classical plate theory (CPT) of Kirchhoff [1] also called Kirchhoff plate theory (KPT) which first employed and developed by Tsiatas [2] to the static bending analysis of microplates. The CPT provides accurate results for analysis of thin plates (length-to-thickness ratios larger than 20) made by homogeneous isotropic materials but, underestimates bending analysis and overestimates vibration analysis of moderately thick plates due to the ignoring shear deformation effects. An extension of KPT is the Mindlin-Reissner theory which was proposed by Mindlin [3] and similarly, but not identical, was proposed by Reissner [4]. Their theory so called first order shear deformation theory (FSDT) or Mindlin plate theory (MPT) which was taken into account the shear deformation effects through the thickness of the plates which is applicable for both thin and moderately thick plates [5]. The challenges related to the FSDT are the inaccurate distribution of transverse shear stress and strain and also the violation of traction free boundary conditions at the top and bottom surfaces of the plate, which to adjust the shear stress distribution, the shear correction factor is required which makes this theory inconvenient to be used. Reddy [6] presented third order shear deformation theory (TSDT) so called Reddy plate theory (RPT) to avoid shear correction factor by the aim of using cubic term in the thickness coordinate in the proposed displacement field, hence the transverse shear strain and stress are represented as quadratic through the thickness, and vanish on the top and bottom surfaces of the plate. CPT, FSDT and TSDT are commonly used theories in the literatures, but other higher order theories are assumed and proposed by other researchers such as sinusoidal shear deformable theory (SSDT) of Touratier [7], the hyperbolic shear deformable plate theory of Soldatos (HSDPT) [8], the trigonometric shear deformable plate theory (TSDPT) of Ferreira et al. [9], exponential shear deformation theory (ESDT) of Karama [10] or parabolic shear deformation theory (PSDT) and some other refined plate theories [5,11] which each one contains different assumptions and significant advantages.

By defining mentioned theories, many researchers try to use them to analyze the bending behavior of plates with different shapes under various conditions. So, among the literatures different studies could be found that by the aim of classical plate theory (CPT) [12,13], first order shear deformation theory (FSDT) [13,14], third order shear deformation theory (TSDT) [15] or higher order shear deformation theory (HSDT) [16] devoted to analyze the bending behavior of axisymmetric circular plates. But, few studies are examined the bending of circular plates based on 3D elasticity theory such as ones by Yang et al. [17] recently, which investigated 3D bending of axisymmetric functionally graded (FG) graphene reinforced circular and annular plates.

Among the literature, few studies examined the asymmetric bending of circular plates. Tielking [18] investigated asymmetric bending of an isotropic, variable thickness annular plate with clamped edges using Von Karman plate theory and Ritz method. Pardoen [19] examined asymmetric bending of circular plates subjected to a concentrated force using the finite element method. Al Jarboubh Ali [20] presented a mechanical modelling for the behavior of the metallic circular plate under the effect of asymmetric loading. However, by the knowledge of the authors, no study is found which investigated the nonlinear bending of plates with asymmetric boundary conditions based on 3D elasticity theory.

In this study, the nonlinear bending analysis of orthotropic annular and circular plates with asymmetric boundary conditions based on 3D elasticity theory is investigated for the first time. For this purpose, the SAPM as a new numerical method, which is presented by the authors recently [14], is used to solve the obtained equations. Dastjerdi and Jabbarzadeh [14-16] presented and used SAPM to solve the symmetric bending of plates based on different theories except 3D elasticity. While, the SAPM is a simple and powerful numerical method with various potentials, which one of them is the potentiality of, solving governing equations related to the 3D bending analysis of plates with asymmetric boundary conditions that this potentiality will be discussed in this study. For this purpose, initially the governing equations of nonlinear bending of orthotropic annular and circular plates based on 3D elasticity theory using principle of stationary total potential energy is derived. Secondly, the boundaries of the plate are divided to two or three parts and different boundary conditions is employed to each part. Two types of asymmetry is considered: (a) asymmetry through one direction, which means that the inner and outer radius have the same boundary conditions at each part and the asymmetry is through θ direction, and (b) asymmetry through two directions, which means that the inner and outer radius boundary conditions at each part have different boundary conditions and the asymmetry is through r and θ directions. The analysis is performed for different types of loading such as mechanical, thermal and thermo-mechanical, and the influence of elastic foundations under different boundaries is investigated.

It is observed that the obtained results are in good agreement with the results reported in the literatures (in symmetry case) and the FEM results (in asymmetry cases). In addition, it is concluded that the 3D elasticity theory estimates higher values of deflections than other theories of plates such as CPT, FSDT and TSDT. The obtained results by 3D elasticity theory and those obtained by FEM analysis in the case of asymmetric conditions are so close.

2 GOVERNING EQUATIONS

2.1 3D elasticity theory formulation

A schematic of an annular plate is shown in Fig.1 with inner radius r_i , outer radius r_o , and thickness of h under uniform transverse loading q resting on two parameters Winkler-Pasternak elastic foundation. k_w and k_p are the Winkler and Pasternak stiffness coefficients of elastic foundation respectively.

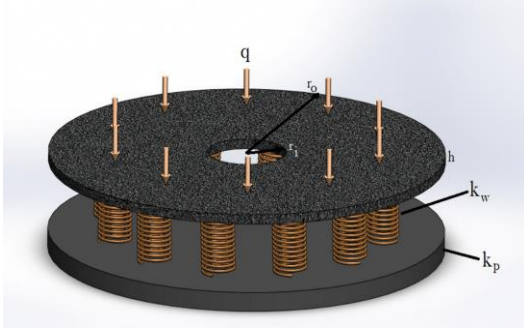


Fig.1
The schematic view of an annular/circular plate under uniform loading and rested on elastic foundation.

According to the 3D elasticity theory of plates, the displacements filed can be expressed as follow:

$$u_1(r, \theta, z) = u(r, \theta, z) \tag{1}$$

$$u_2(r, \theta, z) = v(r, \theta, z) \tag{2}$$

$$u_3(r, \theta, z) = w(r, \theta, z) \tag{3}$$

where u_i is the displacement vector and u, v, w are the displacement components along the r, θ, z directions respectively. It is obvious that no assumption or simplification is employed in definition of displacement vectors. To investigate the mechanical bending analysis, the following Von-Karman strain equation is used [21]:

$$\varepsilon_{ij} = \frac{1}{2}(u_{i,j} + u_{j,i} + u_{k,i}u_{k,j}) \tag{4}$$

where ε_{ij} is the stress tensor and to define the thermal stress following relation is used [21]:

$$\varepsilon_T = \alpha \Delta T \tag{5}$$

where ε_T is the thermal strain α is thermal diffusivity and ΔT is the temperature difference.

By substituting Eqs. (1)- (3) into Eq. (4) and defining ε_T using Eq. (5), the nonlinear components of the Von-Karman strain field can be written as:

$$\varepsilon_{rr} = \frac{\partial u}{\partial r} + \frac{1}{2} \left(\frac{\partial w}{\partial r} \right)^2 - \alpha \Delta T \tag{6}$$

$$\varepsilon_{\theta\theta} = \frac{u}{r} + \frac{1}{r} \frac{\partial v}{\partial \theta} + \frac{1}{2} \left(\frac{1}{r} \frac{\partial w}{\partial \theta} \right)^2 - \alpha \Delta T \tag{7}$$

$$\varepsilon_{zz} = \frac{\partial w}{\partial z} + \frac{1}{2} \left(\frac{\partial w}{\partial z} \right)^2 - \alpha \Delta T \tag{8}$$

$$\varepsilon_{r\theta} = \frac{1}{2} \left(\frac{1}{r} \frac{\partial u}{\partial \theta} + \frac{\partial v}{\partial r} - \frac{v}{r} + \frac{1}{r} \frac{\partial w}{\partial r} \frac{\partial w}{\partial \theta} \right) \quad (9)$$

$$\varepsilon_{\theta z} = \frac{1}{2} \left(\frac{\partial v}{\partial z} + \frac{1}{r} \frac{\partial w}{\partial \theta} + \frac{1}{r} \frac{\partial w}{\partial \theta} \frac{\partial w}{\partial z} \right) \quad (10)$$

$$\varepsilon_{rz} = \frac{1}{2} \left(\frac{\partial u}{\partial z} + \frac{\partial w}{\partial r} + \frac{\partial w}{\partial r} \frac{\partial w}{\partial z} \right) \quad (11)$$

Due to the orthotropic behavior of employed plate, the stress-strain relations using Hook's law [22] are derived as:

$$\sigma_{rr} = \frac{E_r}{\kappa} \left[(1 - \nu_{\theta z} \nu_{z\theta}) \varepsilon_{rr} + (\nu_{\theta r} + \nu_{\theta z} \nu_{zr}) \varepsilon_{\theta\theta} + (\nu_{zr} + \nu_{\theta r} \nu_{z\theta}) \varepsilon_{zz} + ((1 - \nu_{\theta z} \nu_{z\theta})(\nu_{\theta r} + \nu_{\theta z} \nu_{zr})(\nu_{zr} + \nu_{\theta r} \nu_{z\theta})) \alpha \Delta T \right] \quad (12)$$

$$\sigma_{\theta\theta} = \frac{E_r}{\kappa} \left[(\nu_{r\theta} + \nu_{rz} \nu_{z\theta}) \varepsilon_{rr} + (1 - \nu_{rz} \nu_{zr}) \varepsilon_{\theta\theta} + (\nu_{z\theta} + \nu_{r\theta} \nu_{zr}) \varepsilon_{zz} + ((\nu_{r\theta} + \nu_{rz} \nu_{z\theta})(1 - \nu_{rz} \nu_{zr})(\nu_{z\theta} + \nu_{r\theta} \nu_{zr})) \alpha \Delta T \right] \quad (13)$$

$$\sigma_{zz} = \frac{E_r}{\kappa} \left[(\nu_{rz} + \nu_{r\theta} \nu_{\theta z}) \varepsilon_{rr} + (\nu_{\theta z} + \nu_{rz} \nu_{\theta r}) \varepsilon_{\theta\theta} + (1 - \nu_{r\theta} \nu_{\theta r}) \varepsilon_{zz} + ((\nu_{rz} + \nu_{r\theta} \nu_{\theta z})(\nu_{\theta z} + \nu_{rz} \nu_{\theta r})(1 - \nu_{r\theta} \nu_{\theta r})) \alpha \Delta T \right] \quad (14)$$

$$\sigma_{rz} = G_{rz} \gamma_{rz} \quad (15)$$

$$\sigma_{\theta z} = G_{\theta z} \gamma_{\theta z} \quad (16)$$

$$\sigma_{r\theta} = G_{r\theta} \gamma_{r\theta} \quad (17)$$

where σ_{ij} are the Cauchy stress tensors, γ_{ij} is shear strain, ν_{ij} is poison ratio, E_r is the elastic modulus in r direction, G_{ij} is the shear modulus of orthotropic plate and $\kappa = 1 - \nu_{\theta z} \nu_{z\theta} - \nu_{r\theta} \nu_{\theta r} - \nu_{rz} \nu_{zr} - \nu_{r\theta} \nu_{\theta z} \nu_{zr} - \nu_{\theta r} \nu_{z\theta} \nu_{rz}$ which it is a coefficient factor [22], $\nu_{\theta r} = \nu_{r\theta} \times E_\theta / E_r$, $\nu_{zr} = \nu_{rz} \times E_z / E_r$ and $\nu_{z\theta} = \nu_{\theta z} \times E_z / E_\theta$. The E_θ and the E_z are the elastic moduli in θ and z directions.

2.2 Constitutive equations

In this study, the constitutive equations and boundary conditions are derived based on the principle of stationary total potential energy [21]:

$$\delta(U - W_{ext}) = 0 \quad (18)$$

where δ is the variation symbol and W_{ext} is the potential of applied forces which contains the effects of transverse loading q and Winkler-Pasternak elastic foundation on the surface of plate. The components of total potential energy are defined as:

$$\delta U = \left(\iiint_V \sigma_{rr} \delta \varepsilon_{rr} + \sigma_{\theta\theta} \delta \varepsilon_{\theta\theta} + \sigma_{zz} \delta \varepsilon_{zz} + \sigma_{rz} \delta \gamma_{rz} + \sigma_{r\theta} \delta \gamma_{r\theta} + \sigma_{\theta z} \delta \gamma_{\theta z} \right) r dr d\theta dz \quad (19)$$

$$\delta W_{ext} = \int_0^{2\pi} \int_{r_i}^{r_o} (q - k_w w + k_p \nabla^2 w) \delta w r dr d\theta \quad (20)$$

where $\nabla^2 = \frac{\partial^2}{\partial r^2} + \frac{1}{r} \frac{\partial}{\partial r} + \frac{1}{r^2} \frac{\partial^2}{\partial \theta^2} + \frac{\partial^2}{\partial z^2}$ is the Laplacian operator.

By substituting Eqs. (6)- (11) into the Eq. (19) and neglecting body forces, 3D equilibrium equations of an orthotropic annular/circular plate are derived as:

$$\delta u = 0 : \frac{\partial \sigma_{rr}}{\partial r} + \frac{1}{r} \frac{\partial \sigma_{r\theta}}{\partial \theta} + \frac{\partial \sigma_{rz}}{\partial z} + \frac{\sigma_{rr} - \sigma_{\theta\theta}}{r} = 0 \tag{21}$$

$$\delta v = 0 : \frac{\partial \sigma_{r\theta}}{\partial r} + \frac{2}{r} \sigma_{r\theta} + \frac{1}{r} \frac{\partial \sigma_{\theta\theta}}{\partial \theta} + \frac{\partial \sigma_{\theta z}}{\partial z} = 0 \tag{22}$$

$$\delta w = 0 : \frac{\partial \sigma_{rz}}{\partial r} + \frac{\sigma_{rz}}{r} + \frac{1}{r} \frac{\partial \sigma_{\theta z}}{\partial \theta} + \frac{\partial \sigma_{zz}}{\partial z} + \frac{1}{r} \frac{\partial}{\partial r} \left(r \sigma_{rr} \frac{\partial w}{\partial r} + \sigma_{r\theta} \frac{\partial w}{\partial \theta} + r \sigma_{rz} \frac{\partial w}{\partial z} \right) + \frac{1}{r} \frac{\partial}{\partial \theta} \left(\sigma_{r\theta} \frac{\partial w}{\partial r} + \frac{\sigma_{\theta\theta}}{r} \frac{\partial w}{\partial \theta} + \sigma_{\theta z} \frac{\partial w}{\partial z} \right) + \frac{1}{r} \frac{\partial}{\partial z} \left(r \sigma_{rz} \frac{\partial w}{\partial r} + \sigma_{\theta z} \frac{\partial w}{\partial \theta} + r \sigma_{zz} \frac{\partial w}{\partial z} \right) = 0 \tag{23}$$

For sake of generality and convenience, the following non-dimensional parameters are introduced [14-16]:

$$\begin{aligned} r^* &= \frac{r}{r_o}, z^* = \frac{z}{r_o}, h^* = \frac{h}{r_o}, u^* = \frac{u}{r_o}, v^* = \frac{v}{r_o}, w^* = \frac{w}{r_o}, q^* = \frac{q}{E_r}, E_r^* = \frac{E_r}{E_r}, E_{\theta}^* = \frac{E_{\theta}}{E_r}, E_z^* = \frac{E_z}{E_r}, G_{rz}^* = \frac{G_{rz}}{E_r} \\ G_{\theta z}^* &= \frac{G_{\theta z}}{E_r}, G_{r\theta}^* = \frac{G_{r\theta}}{E_r}, k_w^* = \frac{k_w \cdot r_o}{E_r}, k_p^* = \frac{k_p}{E_r \cdot r_o} \end{aligned} \tag{24}$$

which to find these non-dimensional parameters is tried to divide each parameter to a parameter with the same dimension. So, all parameters with length dimension are divided to r_o and all elastic modules and foundations are divided to E_r .

In continue as the final step, by substituting Eqs. (6) - (11) into Eqs. (12) - (17) to define the expression of stress components versus the displacement fields and replacing the resulted stress components into the Eqs. (21) - (23) and using non-dimensional parameters, three equilibrium equations are derived as:

$$\begin{aligned} \delta u = 0 : & \frac{\partial}{\partial r^*} \left[\frac{(1 - \nu_{\theta z} \nu_{z\theta})}{\kappa} \left(\frac{\partial u^*}{\partial r^*} + \frac{1}{2} \left(\frac{\partial w^*}{\partial r^*} \right)^2 \right) + \frac{(\nu_{\theta r} + \nu_{\theta z} \nu_{zr})}{\kappa} \left(\frac{u^*}{r^*} + \frac{1}{r^*} \frac{\partial v^*}{\partial \theta^*} + \frac{1}{2} \left(\frac{1}{r^*} \frac{\partial w^*}{\partial \theta^*} \right)^2 \right) + \frac{(\nu_{zr} + \nu_{\theta r} \nu_{z\theta})}{\kappa} \right] + \\ & \left[\frac{\partial w^*}{\partial z^*} + \frac{1}{2} \left(\frac{\partial w^*}{\partial z^*} \right)^2 \right] \\ & \frac{G_{r\theta}^*}{r^*} \frac{\partial}{\partial \theta^*} \left[\frac{1}{r^*} \frac{\partial u^*}{\partial \theta^*} + \frac{\partial v^*}{\partial r^*} - \frac{v^*}{r^*} + \frac{1}{r^*} \frac{\partial w^*}{\partial r^*} \frac{\partial w^*}{\partial \theta^*} \right] + G_{rz}^* \frac{\partial}{\partial z^*} \left(\frac{\partial u^*}{\partial z^*} + \frac{\partial w^*}{\partial r^*} + \frac{\partial w^*}{\partial r^*} \frac{\partial w^*}{\partial z^*} \right) + \\ & \frac{(1 - \nu_{\theta z} \nu_{z\theta})}{\kappa} \frac{1}{r^*} \left(\frac{\partial u^*}{\partial r^*} + \frac{1}{2} \left(\frac{\partial w^*}{\partial r^*} \right)^2 - \alpha \Delta T \right) + \frac{(\nu_{\theta r} + \nu_{\theta z} \nu_{zr})}{\kappa} \frac{1}{r^*} \left(\frac{u^*}{r^*} + \frac{1}{r^*} \frac{\partial v^*}{\partial \theta^*} + \frac{1}{2} \left(\frac{1}{r^*} \frac{\partial w^*}{\partial \theta^*} \right)^2 - \alpha \Delta T \right) + \\ & \frac{(\nu_{zr} + \nu_{\theta r} \nu_{z\theta})}{\kappa} \frac{1}{r^*} \left(\frac{\partial w^*}{\partial z^*} + \frac{1}{2} \left(\frac{\partial w^*}{\partial z^*} \right)^2 - \alpha \Delta T \right) - \frac{1}{r^*} \left(\frac{(1 - \nu_{\theta z} \nu_{z\theta})(\nu_{\theta r} + \nu_{\theta z} \nu_{zr})(\nu_{zr} + \nu_{\theta r} \nu_{z\theta})}{\kappa} \right) \alpha \Delta T - \\ & \frac{(\nu_{r\theta} + \nu_{rz} \nu_{z\theta})}{\kappa} \frac{1}{r^*} \left(\frac{\partial u^*}{\partial r^*} + \frac{1}{2} \left(\frac{\partial w^*}{\partial r^*} \right)^2 - \alpha \Delta T \right) - \frac{(1 - \nu_{rz} \nu_{zr})}{\kappa} \frac{1}{r^*} \left(\frac{u^*}{r^*} + \frac{1}{r^*} \frac{\partial v^*}{\partial \theta^*} + \frac{1}{2} \left(\frac{1}{r^*} \frac{\partial w^*}{\partial \theta^*} \right)^2 - \alpha \Delta T \right) - \\ & \frac{(\nu_{z\theta} + \nu_{r\theta} \nu_{zr})}{\kappa} \frac{1}{r^*} \left(\frac{\partial w^*}{\partial z^*} + \frac{1}{2} \left(\frac{\partial w^*}{\partial z^*} \right)^2 - \alpha \Delta T \right) + \frac{1}{r^*} \left(\frac{(\nu_{r\theta} + \nu_{rz} \nu_{z\theta})(1 - \nu_{rz} \nu_{zr})(\nu_{z\theta} + \nu_{r\theta} \nu_{zr})}{\kappa} \right) \alpha \Delta T = 0 \end{aligned} \tag{25}$$

$\delta v = 0$:

$$G_{r\theta}^* \frac{\partial}{\partial r^*} \left[\frac{1}{r^*} \frac{\partial u^*}{\partial \theta} + \frac{\partial v^*}{\partial r^*} - \frac{v^*}{r^*} + \frac{1}{r^*} \frac{\partial w^*}{\partial r^*} \frac{\partial w^*}{\partial \theta} \right] + G_{r\theta}^* \frac{2}{r^*} \left[\frac{1}{r^*} \frac{\partial u^*}{\partial \theta} + \frac{\partial v^*}{\partial r^*} - \frac{v^*}{r^*} + \frac{1}{r^*} \frac{\partial w^*}{\partial r^*} \frac{\partial w^*}{\partial \theta} \right] +$$

$$\frac{1}{r^*} \frac{\partial}{\partial \theta} \left[\frac{(v_{r\theta} + v_{rz} v_{z\theta})}{\kappa} \left(\frac{\partial u^*}{\partial r^*} + \frac{1}{2} \left(\frac{\partial w^*}{\partial r^*} \right)^2 \right) + \frac{(1 - v_{rz} v_{zr})}{\kappa} \left(\frac{u^*}{r^*} + \frac{1}{r^*} \frac{\partial v^*}{\partial \theta} + \frac{1}{2} \left(\frac{1}{r^*} \frac{\partial w^*}{\partial \theta} \right)^2 \right) \right] +$$

$$\left[\frac{(v_{z\theta} + v_{r\theta} v_{zr})}{\kappa} \left(\frac{\partial w^*}{\partial z^*} + \frac{1}{2} \left(\frac{\partial w^*}{\partial z^*} \right)^2 \right) \right] + \quad (26)$$

$$G_{\theta z}^* \frac{\partial}{\partial z^*} \left(\frac{\partial v^*}{\partial z^*} + \frac{1}{r^*} \frac{\partial w^*}{\partial \theta} + \frac{1}{r^*} \frac{\partial w^*}{\partial \theta} \frac{\partial w^*}{\partial z^*} \right) = 0$$

$\delta w = 0$:

$$G_{rz}^* \frac{\partial}{\partial r^*} \left(\frac{\partial u^*}{\partial z^*} + \frac{\partial w^*}{\partial r^*} + \frac{\partial w^*}{\partial r^*} \frac{\partial w^*}{\partial z^*} \right) + \frac{G_{rz}^*}{r^*} \frac{\partial}{\partial r^*} \left(\frac{\partial u^*}{\partial z^*} + \frac{\partial w^*}{\partial r^*} + \frac{\partial w^*}{\partial r^*} \frac{\partial w^*}{\partial z^*} \right) + \frac{G_{\theta z}^*}{r^*} \frac{\partial}{\partial \theta} \left(\frac{\partial v^*}{\partial z^*} + \frac{1}{r^*} \frac{\partial w^*}{\partial \theta} + \frac{1}{r^*} \frac{\partial w^*}{\partial \theta} \frac{\partial w^*}{\partial z^*} \right) +$$

$$\frac{\partial}{\partial z^*} \left[\frac{(v_{rz} + v_{r\theta} v_{\theta z})}{\kappa} \left(\frac{\partial u^*}{\partial r^*} + \frac{1}{2} \left(\frac{\partial w^*}{\partial r^*} \right)^2 \right) + \frac{(v_{\theta z} + v_{rz} v_{\theta r})}{\kappa} \left(\frac{u^*}{r^*} + \frac{1}{r^*} \frac{\partial v^*}{\partial \theta} + \frac{1}{2} \left(\frac{1}{r^*} \frac{\partial w^*}{\partial \theta} \right)^2 \right) \right] +$$

$$\left[\frac{(1 - v_{r\theta} v_{\theta r})}{\kappa} \left(\frac{\partial w^*}{\partial z^*} + \frac{1}{2} \left(\frac{\partial w^*}{\partial z^*} \right)^2 \right) \right] +$$

$$\frac{\partial}{\partial r^*} \left[\frac{(1 - v_{\theta z} v_{z\theta})}{\kappa} \left(\frac{\partial u^*}{\partial r^*} + \frac{1}{2} \left(\frac{\partial w^*}{\partial r^*} \right)^2 \right) + \frac{(v_{\theta r} + v_{\theta z} v_{zr})}{\kappa} \left(\frac{u^*}{r^*} + \frac{1}{r^*} \frac{\partial v^*}{\partial \theta} + \frac{1}{2} \left(\frac{1}{r^*} \frac{\partial w^*}{\partial \theta} \right)^2 \right) \right] +$$

$$\left[\frac{(v_{zr} + v_{\theta r} v_{z\theta})}{\kappa} \left(\frac{\partial w^*}{\partial z^*} + \frac{1}{2} \left(\frac{\partial w^*}{\partial z^*} \right)^2 \right) \right] \cdot r^* \frac{\partial w^*}{\partial r^*} \quad (27)$$

$$+ G_{r\theta}^* \frac{\partial}{\partial r^*} \left[\left(\frac{1}{r^*} \frac{\partial u^*}{\partial \theta} + \frac{\partial v^*}{\partial r^*} - \frac{v^*}{r^*} + \frac{1}{r^*} \frac{\partial w^*}{\partial r^*} \frac{\partial w^*}{\partial \theta} \right) \frac{\partial w^*}{\partial \theta} \right] + G_{rz}^* \frac{\partial}{\partial r^*} \left[\left(\frac{\partial u^*}{\partial z^*} + \frac{\partial w^*}{\partial r^*} + \frac{\partial w^*}{\partial r^*} \frac{\partial w^*}{\partial z^*} \right) \cdot r^* \frac{\partial w^*}{\partial z^*} \right] +$$

$$G_{r\theta}^* \frac{\partial}{\partial \theta} \left[\left(\frac{1}{r^*} \frac{\partial u^*}{\partial \theta} + \frac{\partial v^*}{\partial r^*} - \frac{v^*}{r^*} + \frac{1}{r^*} \frac{\partial w^*}{\partial r^*} \frac{\partial w^*}{\partial \theta} \right) \frac{\partial w^*}{\partial r^*} \right] + G_{\theta z}^* \frac{\partial}{\partial \theta} \left[\left(\frac{\partial v^*}{\partial z^*} + \frac{1}{r^*} \frac{\partial w^*}{\partial \theta} + \frac{1}{r^*} \frac{\partial w^*}{\partial \theta} \frac{\partial w^*}{\partial z^*} \right) \frac{\partial w^*}{\partial z^*} \right] +$$

$$\frac{1}{r^*} \frac{\partial}{\partial \theta} \left[\frac{(v_{r\theta} + v_{rz} v_{z\theta})}{\kappa} \left(\frac{\partial u^*}{\partial r^*} + \frac{1}{2} \left(\frac{\partial w^*}{\partial r^*} \right)^2 \right) + \frac{(1 - v_{rz} v_{zr})}{\kappa} \left(\frac{u^*}{r^*} + \frac{1}{r^*} \frac{\partial v^*}{\partial \theta} + \frac{1}{2} \left(\frac{1}{r^*} \frac{\partial w^*}{\partial \theta} \right)^2 \right) \right] +$$

$$\left[\frac{(v_{z\theta} + v_{r\theta} v_{zr})}{\kappa} \left(\frac{\partial w^*}{\partial z^*} + \frac{1}{2} \left(\frac{\partial w^*}{\partial z^*} \right)^2 \right) \right] \frac{\partial w^*}{\partial \theta}$$

$$+ G_{rz}^* \frac{\partial}{\partial z^*} \left[\left(\frac{\partial u^*}{\partial z^*} + \frac{\partial w^*}{\partial r^*} + \frac{\partial w^*}{\partial r^*} \frac{\partial w^*}{\partial z^*} \right) \cdot r^* \frac{\partial w^*}{\partial r^*} \right] + G_{\theta z}^* \frac{\partial}{\partial z^*} \left[\left(\frac{\partial v^*}{\partial z^*} + \frac{1}{r^*} \frac{\partial w^*}{\partial \theta} + \frac{1}{r^*} \frac{\partial w^*}{\partial \theta} \frac{\partial w^*}{\partial z^*} \right) \frac{\partial w^*}{\partial \theta} \right] +$$

$$\frac{\partial}{\partial z^*} \left[\frac{(v_{rz} + v_{r\theta} v_{\theta z})}{\kappa} \left(\frac{\partial u^*}{\partial r^*} + \frac{1}{2} \left(\frac{\partial w^*}{\partial r^*} \right)^2 \right) + \frac{(v_{\theta z} + v_{rz} v_{\theta r})}{\kappa} \left(\frac{u^*}{r^*} + \frac{1}{r^*} \frac{\partial v^*}{\partial \theta} + \frac{1}{2} \left(\frac{1}{r^*} \frac{\partial w^*}{\partial \theta} \right)^2 \right) \right] +$$

$$\left[\frac{(1 - v_{r\theta} v_{\theta r})}{\kappa} \left(\frac{\partial w^*}{\partial z^*} + \frac{1}{2} \left(\frac{\partial w^*}{\partial z^*} \right)^2 \right) \right] \cdot r^* \frac{\partial w^*}{\partial z^*} = 0$$

3 SOLUTIONS PROCEDURE

According to the three equilibrium equations, it can be seen that a system of nonlinear partial differential equations is obtained. In this study a new semi-analytical polynomial method (SAPM) which is presented by Dastjerdi and

Jabbarzadeh [14] recently in 2D is employed which can solve the system of nonlinear partial differential equations needless to any assumptions or simplifications. This method is identified by Dastjerdi and Jabbarzadeh [14-16] just as a powerful method, which can solve system of partial equations simply. However, the authors by more studies found more abilities in this method. It is found that this method has potentiality of solving obtained equations for asymmetric conditions about 3D conditions. No numerical method is found that have the ability of solving of all types of systems of partial equation related to the 3D bending of circular plates with all boundary conditions under symmetric and asymmetric conditions. The main purpose of this study is examination and identifying the ability of this solution method in solving 3D bending of plates under asymmetric conditions. To investigate the ability of this method in solving of partial equations related to the symmetric 3D bending of plates, the results are compared with the results in the literatures. However, about asymmetric conditions (due to the lack of results in the literatures), a FE model in ABAQUS software is prepared to examine the accuracy of the obtained results by this method.

In this method, every function in each partial differential equation is estimated by a polynomial in general form depended on the grid point s' distribution. In contrast to the common methods, each polynomial is needless to satisfy boundary conditions. Every partial equation or set of them would be solved conveniently and quickly considering different types of boundary conditions.

By considering a partial differential equation as follows:

$$\begin{aligned} & \frac{\partial^n F(r, \theta, z)}{\partial^n r} + \frac{\partial^{(n-1)} F(r, \theta, z)}{\partial^{(n-1)} r} + \dots + \frac{\partial F(r, \theta, z)}{\partial r} + \frac{\partial^n F(r, \theta, z)}{\partial^n z} + \frac{\partial^{(n-1)} F(r, \theta, z)}{\partial^{(n-1)} z} + \dots + \frac{\partial F(r, \theta, z)}{\partial z} + \frac{\partial^n F(r, \theta, z)}{\partial^n \theta} \\ & + \frac{\partial^{(n-1)} F(r, \theta, z)}{\partial^{(n-1)} \theta} + \dots + \frac{\partial F(r, \theta, z)}{\partial \theta} + \frac{\partial^n F(r, z)}{\partial r \partial^{(n-1)} z} + \frac{\partial^n F(r, z)}{\partial^2 r \partial^{(n-2)} z} + \dots + \frac{\partial^n F(r, z)}{\partial r^{(n-1)} \partial z} + \frac{\partial^n F(r, z)}{\partial r \partial^{(n-1)} \theta} + \frac{\partial^n F(r, z)}{\partial^2 r \partial^{(n-2)} \theta} + \dots + \\ & \frac{\partial^n F(r, z)}{\partial r^{(n-1)} \partial \theta} + \frac{\partial^n F(r, z)}{\partial \theta \partial^{(n-1)} z} + \frac{\partial^n F(r, z)}{\partial^2 \theta \partial^{(n-2)} z} + \dots + \frac{\partial^n F(r, z)}{\partial \theta^{(n-1)} \partial z} + \frac{\partial^n F(r, z)}{\partial r \partial^{(n-1)} z} + \frac{\partial^n F(r, z)}{\partial r \partial \theta \partial^{(n-2)} z} + \frac{\partial^n F(r, z)}{\partial^2 r \partial \theta \partial^{(n-3)} z} + \frac{\partial^n F(r, z)}{\partial^2 r \partial^2 \theta \partial^{(n-4)} z} \\ & + \dots + \frac{\partial^n F(r, z)}{\partial^{(n-2)} r \partial^{(n-2)} \theta \partial^4 z} + \frac{\partial^n F(r, z)}{\partial^{(n-1)} r \partial^{(n-2)} \theta \partial^3 z} + \frac{\partial^n F(r, z)}{\partial^{(n-1)} r \partial^{(n-1)} \theta \partial^2 z} + \frac{\partial^n F(r, z)}{\partial^{(n-1)} r \partial z} = 0 \end{aligned} \tag{28}$$

where the function $F(r, \theta, z)$ is defined as:

$$F(r, \theta, z) = \sum_{i=1}^N \sum_{j=1}^M \sum_{k=1}^P a_i r^{(i-1)} \theta^{(j-1)} z^{(k-1)} \tag{29}$$

where N is the number of grid points in r direction, M is the number of grid points in θ direction and P is the number of grid points in z direction and l is counted from 1 to $N \times M \times P$ by counting i, j, k on the summations, which sample grid point domains are shown in Fig. 2. By substituting Eq. (29) in Eq. (28) the partial differential equation is converted to the algebraic equations which $2M \times P$ number of equations would be derived from boundary conditions (white points) and $(N \times M \times P) - (2M \times P)$ number of equations are derived from Eq. (29) (related to the black points). Consequently, there are $N \times M \times P$ numbers of algebraic equations and unknown a_i coefficients, which by substituting obtained a_i into the Eq. (29), the $F(r, \theta, z)$ function would be determined. For a system of partial differential equations, the similar procedures should be applied.

Due to the above explanations about SAPM, three displacement fields could be defined as follow:

$$u(r, \theta, z) = \sum_{i=1}^N \sum_{j=1}^M \sum_{k=1}^P a_i r^{(i-1)} \theta^{(j-1)} z^{(k-1)} \tag{30}$$

$$v(r, \theta, z) = \sum_{i=1}^N \sum_{j=1}^M \sum_{k=1}^P a_{i+MNP} r^{(i-1)} \theta^{(j-1)} z^{(k-1)} \tag{31}$$

$$w(r, \theta, z) = \sum_{i=1}^N \sum_{j=1}^M \sum_{k=1}^P a_{i+2,MNP} r^{(i-1)} \theta^{(j-1)} z^{(k-1)} \quad (32)$$

which the obtained algebraic equations are solved using numerical methods such as Newton-Raphson method.

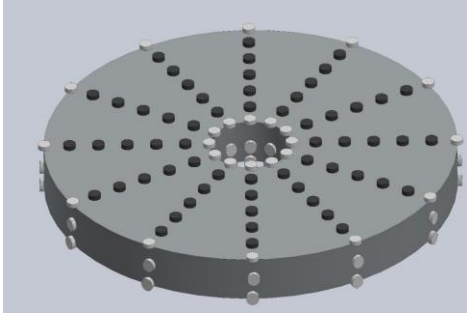


Fig.2
The schematic view of grid points based on SAPM.

4 BOUNDARY CONDITIONS

In the present study, all types of boundary conditions are considered under three categories of the simply supported (S), clamped (C) and free edges (F) which at inner and outer radius (r_i and r_o) the boundary conditions could be defined as follow:

$$S : \sigma_r = v^* = w^* = 0 \quad (33)$$

$$C : u^* = v^* = w^* = 0 \quad (34)$$

$$F : \sigma_r = \sigma_{r\theta} = \sigma_{rz} + \sigma_r \frac{\partial w^*}{\partial r^*} + \frac{1}{r^*} \sigma_{r\theta} \frac{\partial w^*}{\partial \theta} + \sigma_{rz} \frac{\partial w^*}{\partial z^*} = 0 \quad (35)$$

In the present study, to define asymmetric boundary conditions, the plate grid points through θ direction are divided to two (Fig. 3) or three (Fig. 4) categories and each category should satisfy specific boundary condition which this possibility is due to the use of SAPM. As mentioned before, in this method, each polynomial is needless to satisfy boundary conditions and every partial equation or set of them would be solved considering different types of boundary conditions. So, for each part of plate as shown in Figs. 3 and 4 different boundary conditions could be defined.

In addition, the displacement components should satisfy the following boundary conditions at the top and bottom surfaces of plate:

$$\sigma_{rz} \Big|_{z=-\frac{h}{2}}^{\frac{h}{2}} = 0 \quad (36)$$

$$\sigma_{\theta z} \Big|_{z=-\frac{h}{2}}^{\frac{h}{2}} = 0 \quad (37)$$

$$\sigma_{zz} + \sigma_{zz} \frac{\partial w^*}{\partial z^*} + \sigma_{rz} \frac{\partial w^*}{\partial r^*} + \frac{1}{r^*} \sigma_{\theta z} \frac{\partial w^*}{\partial \theta} - q^* \Big|_{z=-\frac{h}{2}} = 0 \quad (38)$$

$$\sigma_{zz} + \sigma_{zz} \frac{\partial w^*}{\partial z^*} + \sigma_{rz} \frac{\partial w^*}{\partial r^*} + \frac{1}{r^*} \sigma_{\theta z} \frac{\partial w^*}{\partial \theta} + k_w^* w^* - k_p^* \left(\frac{\partial^2 w^*}{\partial r^{*2}} + \frac{1}{r^*} \frac{\partial w^*}{\partial r^*} + \frac{\partial^2 w^*}{\partial z^{*2}} \right) \Big|_{z=\frac{h}{2}} = 0 \quad (39)$$

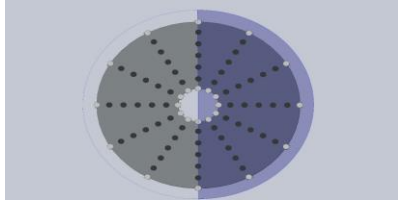


Fig.3
The schematic view of dividing the plate to two parts for defining asymmetric boundary conditions.

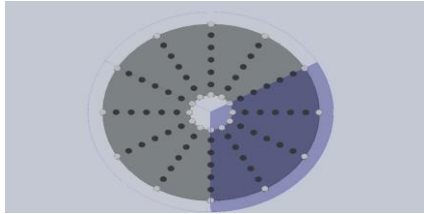


Fig.4
The schematic view of dividing the plate to three parts for defining asymmetric boundary conditions.

5 NUMERICAL RESULTS AND DISCUSSIONS

To investigate the convergence of the SAPM results for different grid numbers, an isotropic annular plate with following properties [10] is considered for different symmetric boundary conditions, which the results are reported in Table 1:

$$E_r = E_\theta = E_z = 2MPa; \nu_{ij} = 0.3; r_i^* = 0.2; h^* = 0.1; q^* = 0.1 \tag{40}$$

Table 1
Convergence checking of non-dimensional deflections of an isotropic annular plate versus the number of grid points.

n (number of domain nodes)	w*					
	Boundary Condition Type					
	C - C	S - S	C - S	S - C	F - C	F - S
5	1.3429	5.5518	3.1683	2.2380	-	-
7	1.4119	5.4942	3.1759	2.2870	-	-
9	1.4390	5.4768	3.2134	2.2917	20.2673	85.6911
11	1.4510	5.4581	3.2151	2.2901	18.3913	82.8252
13	1.4571	5.4552	3.2186	2.2899	18.0180	81.2390

It is considered that the convergence at 13 grid points through r direction is occurred. For all cases, the number of grid points through θ, z directions are 5 points for this part (axisymmetric conditions) but about asymmetric boundary conditions due to the asymmetry directions and the amounts of parts, different number of grid numbers are used to convergence of the results to FE model.

Due to the lack of the results for asymmetric boundary conditions, the validation of the method is performed through the analysis by symmetric boundaries and then the analysis with asymmetric boundaries is investigated. So, as the first step of validation, the deflection of an isotropic circular plate with the following properties for symmetric clamped edges is comprised with Refs. [21, 23-25] in Table 2:

$$E_r = E_\theta = E_z = 2MPa; \nu_{ij} = 0.3; h^* = 0.1 \tag{41}$$

Table 2
Comparison of the non-dimensional deflection of an isotropic circular plate with clamped edges.

q*	$w^* = \frac{w}{r_o} = \frac{12q(1-\nu^2)r_o^3}{64Eh^3}$				
	[23]	[24]	[21]	[25]	Present study
0.0001	0.1685	0.1678	0.1687	0.1706	0.1774
0.0003	0.4642	0.4583	0.4655	0.5119	0.5322
0.001	1.0557	1.0509	1.0937	1.7069	1.7742

which good agreement is observed between the results especially to the Ref. [25]. In addition, the results are compared for an isotropic annular plate for both symmetric clamped and simply supported edges with Refs. [23, 26, 27] for following conditions in Table 3:

$$E_r = E_\theta = E_z = 280GPa; \nu_{ij} = 0.288; h^* = 0.15; q^* = 0.054 \quad (42)$$

Table 3

Comparison of the non-dimensional deflection of an isotropic annular plate with clamped and simply supported edges.

Study	w^*	
	Clamped	Simply supported
[23]	2.810	10.633
[26]	2.781	10.623
[27]	2.774	10.572
Present study	3.015	11.406

which good agreement is observed.

For validation of deflection of orthotropic annular plate in the presence of elastic foundations, the results for following properties (non-zero parameters) are compared with those by [23] in Table 4:

$$E_r^* = 1; E_\theta^* = 0.8; E_z^* = 0.03; G_{rz}^* = 0.3; \nu_{ij} = 0.3; h^* = 0.1; r_i^* = 0.2; q^* = 0.0001; k_w = 1.13Pa/m; k_p = 1.13Pa.m \quad (43)$$

Table 4

Comparison of the non-dimensional deflection of an orthotropic annular plate in the presence of elastic foundations.

Boundary condition type	w^*		
	CPT	Ref. [23]	Present study (3D Elasticity)
C - C	0.0030	FSDT 0.0034	0.0031
S - S	-	0.0085	0.0085
C - S	-	0.0065	0.0053
F - C	-	0.026	0.0263

which it is observed that the results show good agreement.

To verify the accuracy of boundary conditions equations, the nonlinear bending analysis of both circular and annular plates with following conditions are compared with the results reported by Reddy et al. [28] in Table 5:

$$E_r = E_\theta = E_z = 1MPa; \nu_{ij} = 0.25; h^* = 0.1 \quad (44)$$

Table 5

Comparison of the non-dimensional deflections of isotropic annular/circular plate for various boundary conditions.

Study	w^*				
	Circular plate ($r_i^* = 0$)		Annular plate ($r_i^* = 0.25$)		
	F - C $q^* = 0.0001$	F - S $q^* = 0.0001$	F - C $q^* = 0.0001$	C - F $q^* = 0.00005$	F - S $q^* = 0.00005$
[28] CPT	0.01757	0.050	0.01624	0.02358	0.04273
[28] FSDT	0.01829	0.050	0.01685	0.02358	-
Present study	0.01822	0.052	0.01761	0.01860	0.04407

At each four part of validations, it shows that the results are in an accurate range. In addition, it is observed that in the most cases, 3D elasticity theory estimated higher deflections than other theories such as CPT, FSDT, TSDT and some analytical solutions. So, the validity of the present method and solution procedure for various symmetric boundary conditions and elastic foundations checked. In continue, the bending analysis for asymmetric boundary conditions is performed. There is no study in the literature, which investigated the bending analysis for asymmetric boundary conditions. Therefore, for each case, the same finite element model in ABAQUS software is produced to check the validity of the results.

To investigate the asymmetric bending of orthotropic annular and circular plates following properties is considered [14-16, 23 and 29]:

$$E_r^* = 1; E_\theta^* = 0.8; E_z^* = 0.03; G_{rz}^* = 0.6; G_{\theta z}^* = 0.5; G_{r\theta}^* = 0.45; \nu_{r\theta} = \nu_{rz} = \nu_{\theta z} = 0.3; \alpha = 2.02 \times 10^{-6} \tag{45}$$

The nonlinear mechanical bending of an annular plate with $h^* = 0.1, r_i^* = 0.2$ and $q^* = 0.0001$ for symmetric and asymmetric boundary conditions is investigated. For symmetric boundary conditions, the clamped and simply supported conditions are employed and for asymmetric boundary conditions, the boundaries are divided to two and three parts and all three types of boundary conditions (clamped, simply supported and free edges) are employed to each part (Table 6).

Table 6

The symmetric and asymmetric non-dimensional deflections of orthotropic annular plate for various boundary conditions with the same boundaries for inner and outer radius at each part.

Method	w^*									
	Symmetric B.Cs		Two parts asymmetric B.Cs			Three parts asymmetric B.Cs				
	C	S	C-S	C-F	S-F	C-C-S	C-S-S	C-C-F	C-S-F	S-S-F
3D elasticity	0.0014	0.0053	0.0054	0.235	0.251	0.0045	0.0051	0.0562	0.0660	0.0762
ABAQUS	0.0014	0.0053	0.0051	0.236	0.254	0.0042	0.0053	0.0578	0.0664	0.0761

For this step, the asymmetry is considered in θ direction and the same inner and outer radius boundary conditions are employed through r direction. For more illustration and as an example, the schematic view of defining of boundary conditions for a plate with two part with one side clamped and one side simply supported edge is presented in Fig. 5. As it is considered, for all of the white grid points on the right part pf the plate, the clamped boundary conditions and for all the grid points on the left part of the plate, the simply supported condition are defined. The results are in good agreement for all types of boundary conditions. From the results, it is considered that by dividing the plate to two parts, a plate with clamped-simply supported (C-S) edges shows less deflection than symmetric simply edge and more than symmetric clamped edge. The free edge shows more deflections besides simply edge than clamped edge. In addition, by increasing the percentage of clamped edge the decreasing effect on the deflection of the other parts is observed. These observations show that in the plates with asymmetry boundary conditions, the boundaries of each part affect the maximum deflection of other parts.

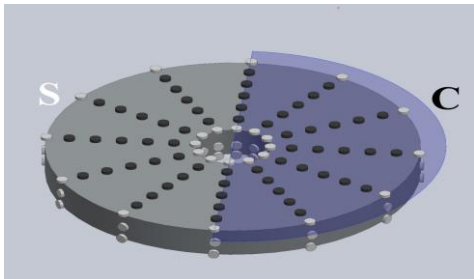


Fig.5
The schematic view of defining of asymmetric clamped-simply supported edges for two part plates.

The nonlinear mechanical bending for the same annular plate with asymmetric boundary conditions by asymmetry through two directions (r and θ directions) is reported in Table 7. The plate is divided to two parts through θ direction and various boundary condition is used for each part. The analyses are under two categories with different inner radius (clamped and simply supported edges). The results of 3D elasticity and FEM (ABAQUS model) show good agreement in this case too and the same influence as last part is considered. When the simply supported inner edge is replaced by clamped inner condition, considerable reduction is considered in the maximum deflection for all types of outer radius boundary conditions.

Table 7

The asymmetric non-dimensional deflections of orthotropic annular plate for various boundary conditions with asymmetry through two directions (two parts).

Method	w^*					
	Simply supported inner radius			Clamped inner radius		
	Outer radius B.Cs			Outer radius B.Cs		
	C-S	C-F	S-F	C-S	C-F	S-F
3D elasticity	0.00542	0.1439	0.1464	0.0030	0.00738	0.00745
ABAQUS	0.00514	0.1407	0.1500	0.0030	0.00736	0.00745

Another nonlinear mechanical bending analysis for the same annular plate with asymmetric boundary conditions by asymmetry through two directions (r and θ directions) is reported in Table 8. The plate is divided to three parts through θ direction and various boundary condition is used for each part. The analyses are under two categories with different inner radius (clamped and simply supported edges). The results are in a same range, which it shows that the asymmetry model and solution procedure presented in this study can simulate the asymmetry bending behavior of annular/circular plates with high accuracy.

To investigate the influence of elastic foundations, the nonlinear bending of the same annular plate with four types of boundary conditions is investigated: (a) asymmetry through θ direction with two parts S-C edges, (b) asymmetry through θ direction with three parts S-C-C edges, (c) asymmetry through θ and r directions with two parts S-C outer edges and S inner edge, and (d) asymmetry through θ and r directions with three parts S-C-C outer edges and C inner edge.

Table 8

The asymmetric non-dimensional deflections of orthotropic annular plate for various boundary conditions with asymmetry through two directions (three parts).

Method	w^*									
	Simply supported inner radius Outer radius B.Cs					Clamped inner radius Outer radius B.Cs				
	C-C-S	C-C-F	C-S-S	S-S-F	C-S-F	C-C-S	C-C-F	C-S-S	S-S-F	C-S-F
3D elasticity	0.00489	0.0850	0.00626	0.0660	0.0587	0.00296	0.0390	0.00302	0.0430	0.0542
ABAQUS	0.00483	0.0852	0.00628	0.0652	0.0603	0.00295	0.0392	0.00306	0.0428	0.0550

The analysis for $k_w^* = 0.001$; $k_p^* = 0.001$ versus the mechanical loading variations is reported in Fig. 6. It is considered that by increasing the loading its nonlinear increasing effect changed to linear increasing effect. Also its increasing influence on deflection in two parts boundary conditions is more than three parts boundary conditions due to the increase in the portion of clamped areas. No considerable different is observed in the case of one or two directions asymmetry about two parts boundary conditions while it is considerable in the case of three parts boundary conditions.

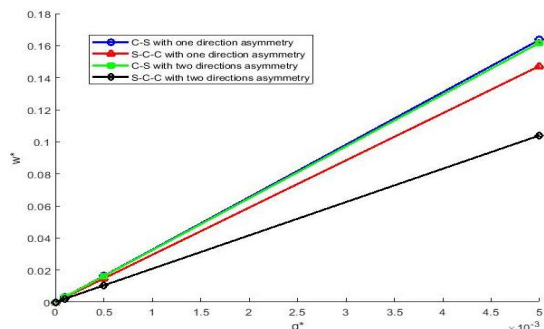


Fig.6

The variation of non-dimensional deflection of orthotropic annular plate rested on elastic foundation versus the loading for various boundary conditions.

Also, the influence of variations of elastic parameters under $q^* = 0.0001$ are illustrated in Figs. 7 and 8. It is observed that by increasing the elastic foundation parameters, the deflection of the plates reduces for all four types of boundary conditions and for both two elastic parameters, and converges to the same value. This convergence is occurred in $k_w^* = 0.01$ which non-dimensional deflections converged to about 0.001 while for Pasternak parameter in $k_p^* = 0.015$ the convergence is observed which reaches to the less than 0.001.

The effect of thermo-mechanical loading on deflection and thickness of the same plate with the same boundary conditions as what used for investigation of influence of elastic parameters, is examined. The variation of non-dimensional deflection and thickness under $k_w^* = 0.01$; $k_p^* = 0.01$; $q^* = 0.0001$ and temperature variations are illustrated in Figs. 9 and 10 respectively. The results show the same linear increasing influence of temperature for all types of boundary conditions. It is considered that the thickness variation versus temperature is not depend on boundary type and condition.

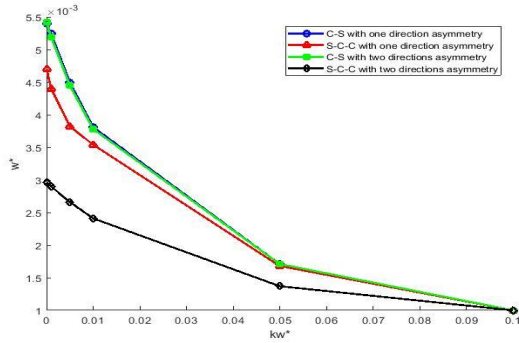


Fig.7
The variation of non-dimensional deflection of orthotropic annular plate versus the Winkler elastic parameter for various boundary conditions.

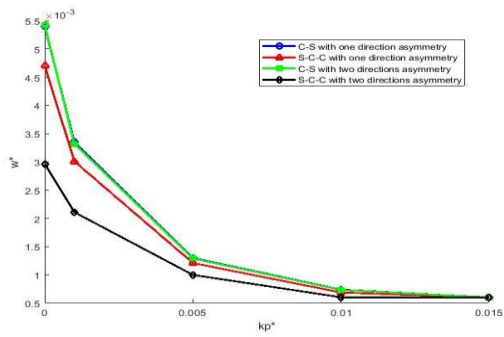


Fig.8
The variation of non-dimensional deflection of orthotropic annular plate versus the Pasternak elastic parameter for various boundary conditions.

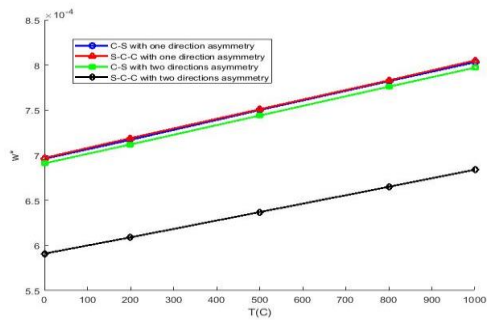


Fig.9
The variation of non-dimensional deflection of orthotropic annular plate versus the temperature for various boundary conditions.

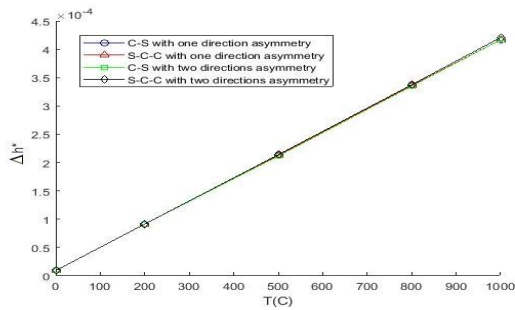


Fig.10
The variation of non-dimensional thickness variation of orthotropic annular plate versus the temperature for various boundary conditions.

6 CONCLUSIONS

In this study, a new numerical solution of asymmetric 3D thermo-mechanical nonlinear bending analysis of orthotropic annular and circular plates using SAPM is presented. The influence of elastic foundations and different boundary conditions is investigated. The asymmetry is due to the employed asymmetric boundary conditions. The plates are divided to two and three parts and two types of asymmetry for each case is considered: the asymmetry

through one and two directions. In one case, the inner and outer radius boundary conditions are the same (on asymmetry direction) and for another, different boundary conditions are used (two asymmetry directions). Due to the lack of study in this case in the literature, the results for symmetric conditions are validated by literature to validate the produced model and solution procedure and the results related to the asymmetry conditions are validated by the aim of FEM. The accuracy of the results shows that the presented 3D model can simulate the bending behavior of the orthotropic annular and circular plates under asymmetric boundary conditions. Due to the agreement of the results, it can be claim that this solutions method is useful to solve the equation related to the 3D bending of plates under asymmetric conditions. It is observed that the 3D elasticity theory estimates higher values of deflections than other theories of plates such as CPT, FSDT and TSDT. Nevertheless, the obtained results by 3D elasticity theory and those obtained by FEM analysis in the case of asymmetric conditions are so close. The influence of temperature is linearly increasing on both deflection and thickness variations. In addition, the deflections in all boundary conditions decreased and reached to the same value by increasing the coefficient of elastic foundations.

REFERENCES

- [1] Kirchhoff G., 1850, Über das Gleichgewicht und die Bewegung einer elastischen Scheibe, *Journal für die Reine und Angewandte Mathematik* **40**: 51-88.
- [2] Tsiatas G.C., 2009, A new Kirchhoff plate model based on a modified couple stress theory, *International Journal of Solids and Structures* **46**(13): 2757-2564.
- [3] Mindlin R.D., 1951, Influence of rotatory inertia and shear on flexural motions of isotropic, elastic plates, *ASME Journal of Applied Mechanics* **18**: 31-38.
- [4] Reissner E., 1945, The effect of transverse shear deformation on the bending of elastic plates, *ASME Journal of Applied Mechanics* **12**: 68-77.
- [5] Lou J., He L., Du J., 2015, A unified higher order plate theory for functionally graded microplates based on the modified couple stress theory, *Composite Structures* **133**: 1036-1047.
- [6] Reddy J.N., 1984, A simple higher-order theory for laminated composite plates, *Journal of Applied Mechanics* **51**(4): 745-752.
- [7] Touratier M., 1991, An efficient standard plate theory, *International Journal of Engineering Science* **29**(8): 901-916.
- [8] Soldatos K., 1992, A transverse shear deformation theory for homogeneous monoclinic plates, *Acta Mechanica* **94** (3): 195-220.
- [9] Ferreira A.J.M., Roque C.M.C., Jorge R.M.N., 2005, Analysis of composite plates by trigonometric shear deformation theory and multiquadratics, *Computers & Structures* **83**(27): 2225-2237.
- [10] Karama M., Afaq K.S., Mistou S., 2003, Mechanical behavior of laminated composite beam by the new multi-layered laminated composite structures model with transverse shear stress continuity, *International Journal of Solids and Structures* **40**(6): 1525-1546.
- [11] Thai H-T., Vo T.P., 2013, A size-dependent functionally graded sinusoidal plate model based on a modified couple stress theory, *Composite Structures* **96**: 376-383.
- [12] Reddy J.N., Berry J., 2012, Nonlinear theories of axisymmetric bending of functionally graded circular plates with modified couple stress, *Computers & Structures* **94**(12): 3664-3668.
- [13] Reddy J.N., Romanoff J., Loya J.A., 2016, Nonlinear finite element analysis of functionally graded circular plates with modified couple stress theory, *European Journal of Mechanics -A/Solids* **56**: 92-104.
- [14] Dastjerdi S., Jabbarzadeh M., 2016, Nonlocal bending analysis of bilayer annular/circular nano plates based on first order shear deformation theory, *Journal of Solid Mechanics* **8**: 645-661.
- [15] Dastjerdi S., Jabbarzadeh M., 2016, Non-local thermo-elastic buckling analysis of multi-layer annular/circular nano-plates based on first and third order shear deformation theories using DQ method, *Journal of Solid Mechanics* **8**: 859-874.
- [16] Dastjerdi S., Abbasi M., Yazdanparast L., 2017, A new modified higher-order shear deformation theory for nonlinear analysis of macro- and nano-annular sector plates using the extended Kantorovich method in conjunction with SAPM, *Acta Mechanica* **228**(10): 3381-3401.
- [17] Yang B., Kitipornchai S., Yang Y.F., Yang J., 2017, 3D Thermo-mechanical bending solution of functionally graded graphene reinforced circular and annular plates, *Applied Mathematical Modelling* **49**: 69-86.
- [18] Tielking J.T., 1979, Asymmetric bending of annular plated, *International Journal of Solids and Structures* **16**: 361-373.
- [19] Pardoen G.C., 1975, Asymmetric bending of circular plates using the finite element method, *Computers & Structures* **5**: 197-202.
- [20] Al Jarboub A., 2015, Mechanical modelling for the behavior of the metallic plate under the effect of bending loads, *Energy Procedia* **74**: 1119-1132.
- [21] Timoshenko S., Woinowsky-Krieger S., 1959, *Theories of Plates and Shells*, New York, McGraw-Book Company.
- [22] Damkilde L., *Continuum Materials*, Aalborg Universitet Esbjerg, IOP Publishing Homes Civil.
- [23] Dastjerdi S., Jabbarzadeh M., 2017, Non-linear bending analysis of multi-layer orthotropic annular/circular graphene sheets embedded in elastic matrix in thermal environment based on non-local elasticity theory, *Applied*

- Mathematical Modelling* **41**: 83-101.
- [24] Altekin M., Yukseler R.F., 2011, *Proceedings of the World Congress on Engineering*, London, U.K.
- [25] Szilard R., 1974, *Theory and Analysis of Plates*, Engle wood Cliffs, Prentice-Hall Inc.
- [26] Reddy J.N., Wang C.M., Kitipornchai S., 1999, Axisymmetric bending of functionally grade circular and annular plates, *European Journal of Mechanics -A/Solids* **18**: 185-199.
- [27] Golmakani M.E., 2013, Non-linear bending analysis of ring-stiffened functionally graded circular plates under mechanical and thermal loadings, *International Journal of Mechanical Sciences* **79**: 130-142.
- [28] Reddy J.N., Romanoff J., Loya J.A., 2016, Nonlinear finite element analysis of functionally graded circular plates with modified couple stress theory, *European Journal of Mechanics -A/Solids* **56**: 92-104.
- [29] Hosseini Kordkheili S.A., Moshrefzadeh-Sani H., 2013, Mechanical properties of double-layered graphene sheets, *Computational Materials Science* **69**: 335-343.